© 2021. Published by The Company of Biologists Ltd | Development (2021) 148, dev197673. doi:10.1242/dev.197673

RESEARCH ARTICLE

The trophoblast clock controls transport across placenta in mice

Cécile Demarez[1], Leonardo Vinicius Monteiro De Assis[1], Markus Krohn[2], Nahuel Ramella[3], Markus Schwaninger[2], Henrik Oster[1] and Mariana Astiz[1,*]

ABSTRACT

In mammals, 24-h rhythms of physiology and behavior are organized by a body-wide network of clock genes and proteins. Despite the well-known function of the adult circadian system, the roles of maternal, fetal and placental clocks during pregnancy are poorly defined. In the mature mouse placenta, the labyrinth zone (LZ) is of fetal origin and key for selective nutrient and waste exchange. Recently, clock gene expression has been detected in LZ and other fetal tissues; however, there is no evidence of a placental function controlled by the LZ clock. Here, we demonstrate that specifically the trophoblast layer of the LZ harbors an already functional clock by late gestation, able to regulate in a circadian manner the expression and activity of the xenobiotic efflux pump, ATP-binding cassette sub-family B member 1 (ABCB1), likely gating the fetal exposure to drugs from the maternal circulation to certain times of the day. As more than 300 endogenous and exogenous compounds are substrates of ABCB1, our results might have implications in choosing the maternal treatment time when aiming either maximal/minimal drug availability to the fetus/mother.

KEY WORDS: Circadian clock, Mice, Placenta, Trophoblast, Xenobiotic efflux transporter

INTRODUCTION

During pregnancy, the mammalian endocrine system promotes maternal metabolic adaptations including enhanced storage of nutrients during the first two-thirds and subsequent acceleration of trans-placental nutrient transport to support fetal growth during the last third (Chourpiliadi and Paparodis, 2020; Russell and Brunton, 2019). The placenta is the only organ that is formed by the interaction of both maternal and fetal/embryonic tissues, providing the interface between their circulatory systems. The placenta regulates essential nutrient and endocrine signal transport, as well as immunological functions that are crucial for fetal development (Sibley and Dilworth, 2020). In rodents, the labyrinth zone (LZ) is a labyrinthine structure with maternal blood spaces separated from the fetal vasculature by trophoblasts and fetal connective tissue. The LZ is of fetal origin and analogous to the chorionic villi in humans (Han et al., 2018). Its main role is to control the exchange of nutrients, hormones, xenobiotics, metabolites and waste between mother and fetus (Han et al., 2018; Staud and Karahoda, 2018). The endocrine system is finely synchronized and coordinated by the circadian system (in 24-h rhythms) ensuring the adaptation of physiology and behavior to daily recurrent changes in the environment. Although little is known in this context, circadian coordination likely plays a fundamental role in pregnancy (Papacleovoulou et al., 2017; Wharfe et al., 2016).

The adult circadian system is organized hierarchically with a master pacemaker located in the hypothalamic suprachiasmatic nucleus (SCN) and subordinated clocks found throughout the brain and periphery (Ralph et al., 1990). The SCN perceives time of day via direct photic input from the retina and subsequently relays temporal information to peripheral clocks, present in almost all cells in the body, by humoral and neuronal pathways (Dibner et al., 2010; Husse et al., 2015; Schibler et al., 2003; So et al., 2009). The molecular circadian clockwork is based on a set of clock genes including *Bmal1* (brain and muscle aryl hydrocarbon receptor nuclear translocator-like 1; also known as *Arntl*), *Per1* and *Per2* (period 1 and 2) and *RevErbα* (reverse erythroblastoma alpha; *Nr1d1*) organized in a system of interlocked transcriptional-translational feedback loops (TTFL) (Gekakis et al., 1998; Shearman et al., 2000; Takahashi, 2017). Time-of-day information is translated into physiological signals through rhythmic regulation of downstream clock-controlled genes (Buhr and Takahashi, 2013). In the context of pregnancy, the circadian coordination would require the interaction between maternal, placental and embryo/fetal clocks, sensing and integrating signals to promote the dynamic and complex process of development in synchrony with the environment (Mark et al., 2017; Astiz and Oster, 2021).

There is already evidence that the circadian system synchronizes maternal metabolic adaptations in the liver to support fetal growth (Papacleovoulou et al., 2017; Wharfe et al., 2016). Meanwhile, the fetal circadian system develops and gains autonomy towards term (Astiz et al., 2020; Landgraf et al., 2015; Wharfe et al., 2011) under the influence of endogenous and exogenous signals crossing the feto-maternal interphase, the placenta (Mendez et al., 2016; Smarr et al., 2017; Varcoe et al., 2011, 2013, 2018; Vilches et al., 2014). Recent evidence has shown clock gene expression in several fetal tissues including the LZ of the placenta by mid gestation in rodents (Čečmanová et al., 2019; Landgraf et al., 2015; Waddell et al., 2012; Crew et al., 2018). However, the functionality of clocks of fetal origin have been questioned as not all the members of the interlocked TTFL are rhythmically expressed in the circadian range, as they are in adult tissues. Therefore, fetal clocks have been considered to be slave oscillators entrained by maternal rhythmic signals crossing placenta (Astiz et al., 2020; Crew et al., 2018; Honma, 2020; Houdek and Sumová, 2014; Mendez et al., 2012; Reppert and Schwartz, 1984; Serón-Ferré et al., 2012). Some of those signals freely cross the placenta (and convey the external time to the fetus) and some others are metabolized by enzymes expressed in the LZ (Christ et al., 2012; Houdek et al., 2016; Krozowski et al., 1999; Mark et al., 2017; Okatani et al., 1998; Waddell et al., 2012).

[1]Institute of Neurobiology, Center of Brain, Behavior and Metabolism (CBBM), University of Lübeck. Marie-Curie-Straße, 23562 Lübeck, Germany. [2]Institute for Experimental and Clinical Pharmacology and Toxicology, Center of Brain, Behavior and Metabolism (CBBM), University of Lübeck. Marie-Curie-Straße, 23562 Lübeck, Germany. [3]Instituto de Investigaciones Bioquímicas de La Plata (INIBIOLP), Facultad de Ciencias Médicas, Universidad Nacional de La Plata, Calles 60 y 120, 1900 La Plata, Argentina.

*Author for correspondence (marianaastiz@gmail.com)

M.K., 0000-0002-5345-9048; M.A., 0000-0001-9912-1686

Handling Editor: Patrick Tam
Received 9 October 2020; Accepted 22 March 2021

Development (2021) 148, dev197673. doi:10.1242/dev.197673

For example, drug efflux transporters such as the ATP-binding cassette sub-family B member 1 (ABCB1) are highly expressed in the placenta to protect the fetus from the accumulation of ABCB1 substrates. More than 300 endogenous and exogenous compounds are substrates of ABCB1, thus it is considered an extremely relevant pharmacological target (Borst and Schinkel, 2013; Genovese et al., 2017). Recent studies have shown that ABCB1 activity shows a circadian rhythm in the intestine (Zhou et al., 2019), affecting the pharmacokinetics and pharmacodynamics of drugs. This is especially relevant in the context of pregnancy, where drug efficacy and toxicity for both the mother and the fetus cannot be well defined.

Therefore, we hypothesize that the clock in the LZ of the placenta regulates the expression and activity of the xenobiotic efflux transporter ABCB1 and that it might gate at certain developmental windows the diurnal exposure of the fetus to its substrates.

RESULTS

The labyrinth zone of the mouse placenta rhythmically expresses clock genes

In order to test our hypothesis, we first determined the presence of a functional clock in the LZ of the placenta during late pregnancy. We mated wild-type C57Bl/6 males and females and dissected placentas and LZ during gestational day (GD) 15-GD15.5 (term is GD19.5) every 6 h to assess the diurnal expression of canonical clock genes (Fig. 1A). *Per2* and *RevErbα* showed rhythmic 24-h expression profiles peaking at the beginning of the dark and the middle of the light phase, respectively (Fig. 1B). We did not, however, find a significant rhythmicity in the expression of other clock genes such as *Bmal1*, *Clock*, *Per1* and *Npas2* (Fig. S1). Using immunohistochemistry, we detected a diurnal variation of BMAL1-positive nuclei in the placental LZ (Fig. 1C). As shown before in several tissues from fetal origin, not all the canonical clock genes are rhythmic around this gestational age (Čečmanová et al., 2019; Li et al., 2012; Mészáros et al., 2014). Nevertheless, the early rhythmic genes (*Per2* and *RevErbα*) or rhythmic maternal entrainment signals could induce the rhythmic expression of downstream targets.

The expression of the xenobiotic efflux transporter ABCB1a/b is induced by glucocorticoids

In those same placentas we assessed the diurnal expression of the two mouse variants of the xenobiotic efflux transporter *Abcb1a* and *Abcb1b* and found a rhythmic 24-h expression profile (Fig. 2A,B). The expression was higher during the dark phase, likely providing the fetus a better protection to xenobiotics during the maternal active phase. However, at least in mice, the expression of these genes is induced by glucocorticoids (GCs), one of the main rhythmic maternal entrainment signals (Lye et al., 2018; Manceau et al., 2012). Indeed, 1 h after a subcutaneous injection of a high dose of corticosterone to pregnant mice at GD15-GD15.5 (Fig. 2C), we found an acute induction of both variants of the gene in the LZ of the placenta (Fig. 2D). Thus, we reasoned that the rhythmic expression of *Abcb1a*/*b* (shown in Fig. 2B) could be an effect of the local clock in the placental LZ, of the maternal GC rhythms peaking at the beginning of the active phase, or of both.

Abcb1a/*b* rhythmic expression depends on the local clock in the placental LZ

In order to dissect the contribution of the local clock in the LZ and the maternal GC rhythms, we used clock-deficient dams (*Per1*/*2* double knockout) mated with wild-type C57Bl/6 males. From this breeding we obtained fetuses heterozygous for *Per1* and *Per2* and, thus, with a functional clock in the LZ of their placentas from dams with no diurnal differences in GC levels (Fig. 3A). During GD15-GD15.5 we collected maternal blood and placentas at ZT1 (1 h after lights on, at the beginning of the maternal resting phase) and at ZT13 (1 h after lights off, at the beginning of the maternal active phase). We checked the maternal GC levels at both time points, and no significant difference was found between ZT1 and ZT13 (Fig. 3B). The levels of plasma corticosterone at ZT13 are two times higher than at ZT1 in wild-type pregnant mice at this gestational age (Fig. S2A). Interestingly, in absence of a difference in the diurnal maternal GC levels, we still found a higher expression of both *Abcb1a* and *Abcb1b* in the LZ of the fetal placenta at ZT13 than at ZT1, indicating that the diurnal regulation is, at least in part, independent of the physiologic maternal production of GCs and, thus, potentially induced by the local clock in the LZ (Fig. 3C). To confirm whether the diurnal regulation of the efflux transporter depends on the local clock in the LZ, we mated male and female mice, which were heterozygous for the clock gene *Bmal1* (+/−). With this breeding combination we obtained, from clock-sufficient dams, homozygous *Bmal1* (+/+) and (−/−) fetuses and, thus, placental LZs with and without a functional clock, respectively (Fig. 4A). We first checked maternal GC levels between ZT1 and ZT13 (Fig. 4B) and found them comparable with the levels in wild-type dams at the same gestational age (Fig. S2A). The expression of *Abcb1a*/*b* was higher at ZT13 in LZ from *Bmal1* (+/+) placentas, but the diurnal difference was not observed in the *Bmal1* (−/−) littermates (Fig. 4C; Fig. S2B-D), indicating that the local clock in the LZ might be responsible for the diurnal regulation of Abcb1 expression. Therefore, we sought to check whether not only the expression of the protein but also the activity was diurnally regulated.

The trophoblast clock controls the rhythmic expression and activity of ABCB1

We first aimed at localizing ABCB1 protein in the mouse LZ during GD15-GD15.5, using double immunofluorescence to detect the protein either in the trophoblast or endothelium layer (Fig. 5). We used cytokeratin (CK) as a marker for the trophoblast layer and CD31 (Pecam1) as a marker of fetal endothelium (both red), anti-ABCB1 antibody (detecting a and b isoforms; green) and DAPI (blue) to label the nuclei (Fig. 5A). The ABCB1 protein co-localizes with CK in the trophoblasts (Fig. 5B) and it shows no co-localization with the fetal endothelium marker CD31 (Fig. 5C). The localization of ABCB1 in the trophoblast layer was previously reported in rodents (Sun et al., 2006) and humans (Han et al., 2018; Novotna et al., 2004). Thus, we reasoned that a trophoblast cell line with a functional molecular clock in which ABCB1 is expressed would be a good model to mechanistically describe the diurnal regulation of ABCB1 activity by the clock. Therefore, we used a human placental trophoblast (BeWo) cell line and first checked whether these cells were able to express clock genes and ABCB1 in a rhythmic fashion. BeWo cells were plated, and after 24 h were synchronized for 2 h with serum shock [50% F12K medium, 50% fetal bovine serum (FBS)] and collected every 6 h to check the circadian rhythmic expression of canonical clock genes over two circadian cycles (Fig. 6A). As observed in LZ from mouse placentas, *PER2*, *REVERBα* and *BMAL1* expression was rhythmic (Fig. 6B). The mRNA expression (Fig. 6C) and the amount of ABCB1 protein (Fig. 6D) in BeWo cells were also rhythmic, showing a peak 30 and 36 h after synchronization, respectively. To assess the role of the trophoblast clock in regulating the circadian activity of ABCB1, we combined an activity assay with a pharmacological disruption of the clock. To quantify the efflux transporter activity, we used calcein-AM as substrate for ABCB1

Development (2021) 148, dev197673. doi:10.1242/dev.197673

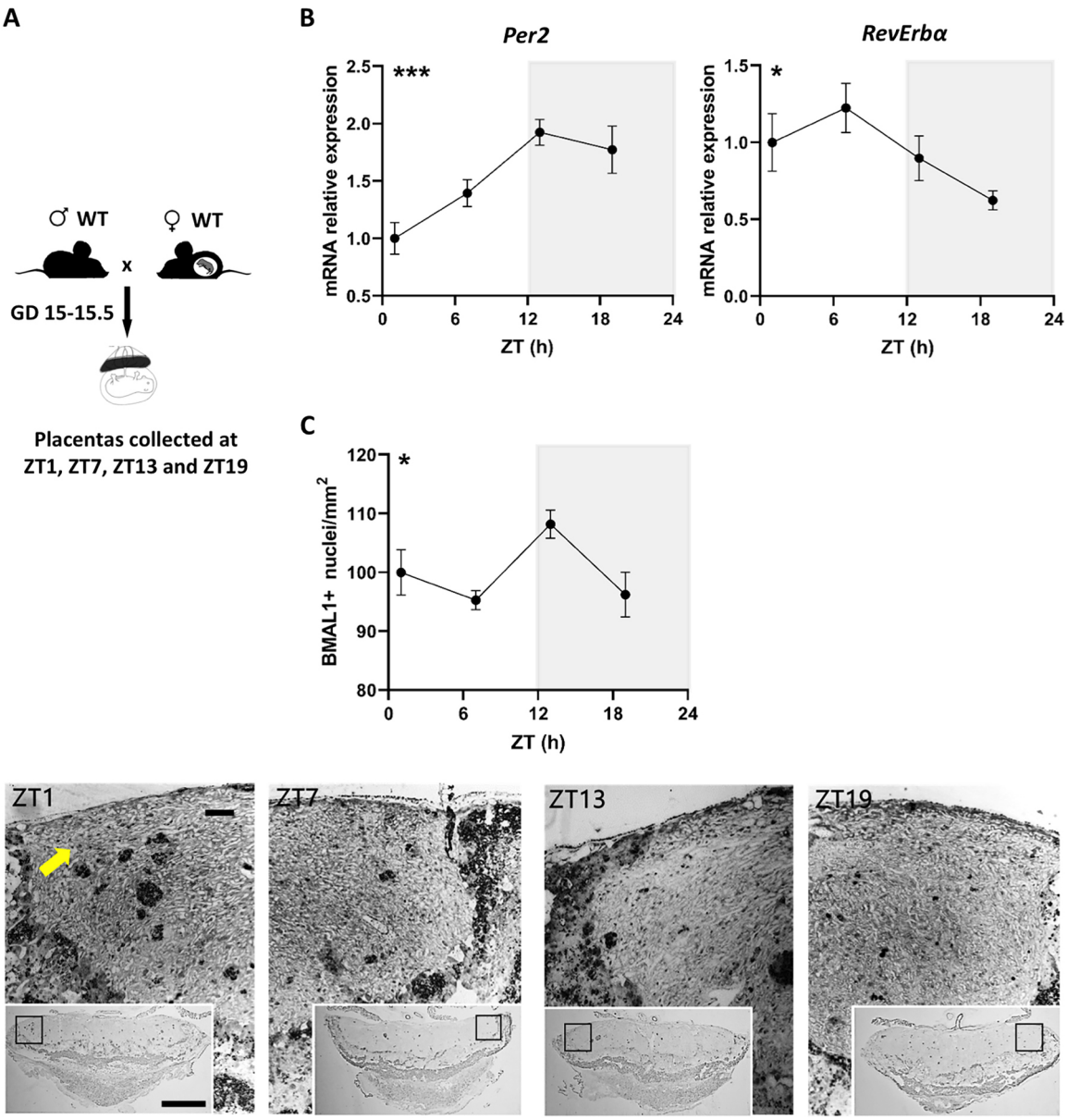

Fig. 1. The labyrinth zone of the mouse placenta rhythmically expresses clock genes. (A) Scheme of sample collection. (B) mRNA relative expression of the clock genes *Per2* and *RevErbα* in the labyrinth zone (LZ) of the placenta. (C) Top: number of BMAL1+ nuclei/mm^2. Bottom: representative images of the immunohistochemistry for BMAL1. Insets show entire placenta (scale bar: 1 mm), boxed area shows the LZ at a higher magnification (scale bar: 100 µm). Yellow arrow points to an example of a BMAL1+ nucleus. Dark gray areas in A-C represent dark phases. Data in B and C are shown as mean±s.e.m. (n=6). *CircWave* software was used to assess circadian rhythmicity by fitting the data to a cosine function and *P*-values represents the statistical significance of that fit. **P*<0.05, ****P*<0.001. ZT, Zeitgeber time.

(Glavinas et al., 2011). If no ABCB1 is expressed, most of the calcein-AM passively permeates into the cells where it is hydrolyzed by cellular esterases into calcein emitting a fluorescent signal. However, if ABCB1 is expressed and active, calcein-AM will be pumped out from the plasma membrane before entering the cell. Thus, the inhibition of ABCB1 activity (e.g. with PCS833) leads to the maximum increase of intracellular fluorescence. We used the difference between the increase of fluorescence in cells treated with and without PSC833 to assess ABCB1-specific activity, measured every 6 h in cells incubated with or without SR8278, an antagonist of REVERBα (Fig. 6E). The antagonist effect of SR8278 in our experimental set up was validated by the evaluation of *BMAL1* expression (main target of REVERBα) after synchronization. In the presence of the antagonist we achieved a stable and non-rhythmic expression of *BMAL1* during the whole time-frame in which ABCB1 activity was measured, indicating the absence of circadian gene expression under these conditions (Fig. 6F). The activity of ABCB1 measured over 24 h showed a circadian variation that was absent when the circadian clock was disrupted by pre-treating with SR8278, confirming a trophoblast-clock dependent mechanism (Fig. 6G).

DISCUSSION

Using a combination of *in vivo* and *in vitro* experiments, we investigated the role of the clock in the LZ of the placenta as a possible regulator of the expression and activity of ABCB1. Our results show, for the first time, a function of the local clock in the trophoblasts, regulating the activity of this placental transporter in a diurnal manner, which might protect the fetus from xenobiotics

Development (2021) 148, dev197673. doi:10.1242/dev.197673

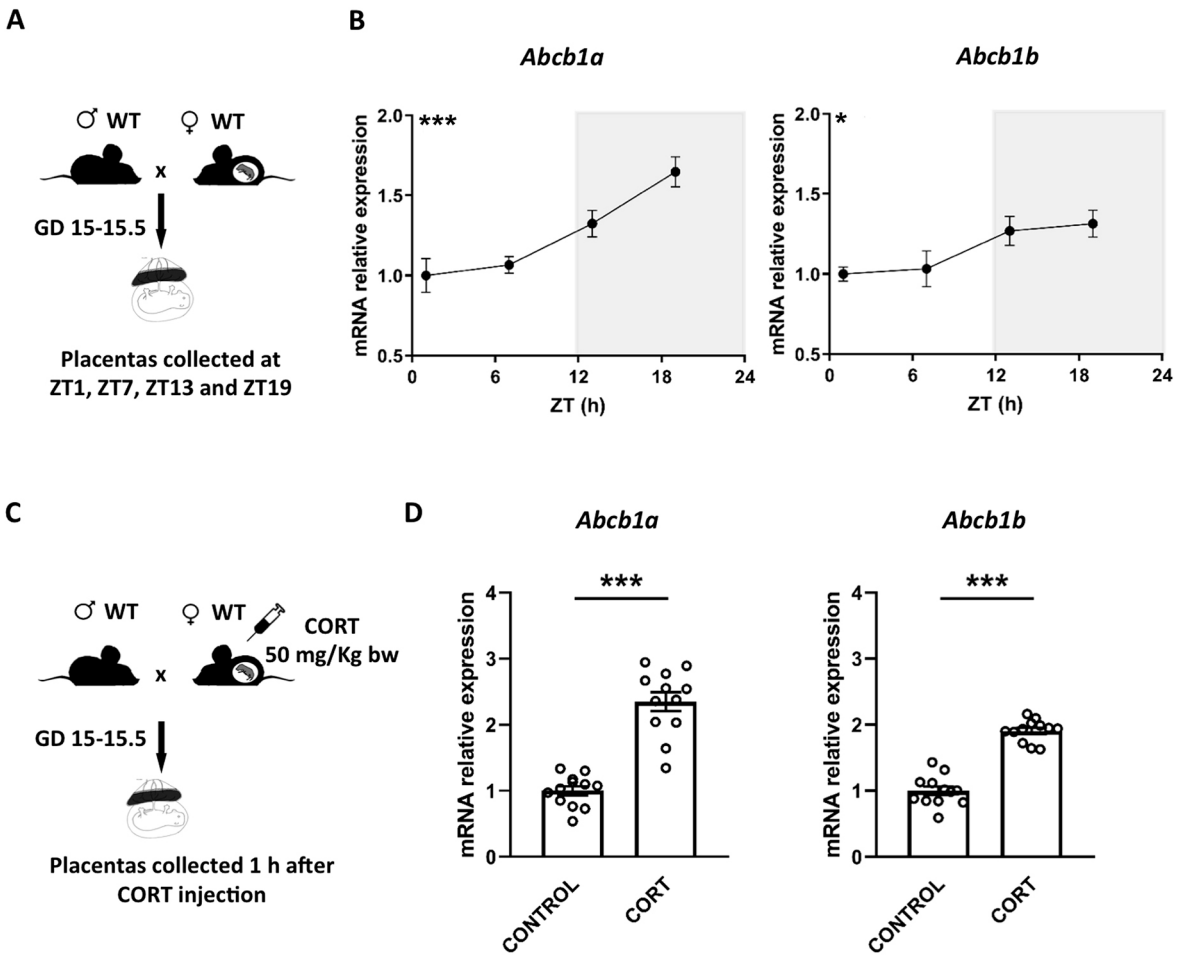

Fig. 2. The expression of the xenobiotic efflux transporter ABCB1a/b is induced by glucocorticoids. (A) Scheme of sample collection. (B) Relative mRNA expression of *Abcb1a* and *Abcb1b* in the labyrinth zone (LZ) of the placenta from samples collected as described in A. Dark gray areas represent dark phases. (C) Scheme of sample collection 1 h after maternal corticosterone (CORT; 50 mg/kg body weight) subcutaneous injection. (D) Relative mRNA expression in the LZ of the placenta from samples collected as described in C. Data in B are shown as mean±s.e.m. (n=6). *CircWave* software was used to assess circadian rhythmicity by fitting the data to a cosine function and P-values represent the statistical significance of that fit. *P<0.05, ***P<0.001. Data in D are shown as mean±s.e.m. (n=12). Data were analyzed by two-sided unpaired t-test (*Abcb1a*, t=8.4, d.f.=22, ***P<0.0001; *Abcb1b*, t=11.1, d.f.=22, ***P<0.0001).

during the maternal active phase when the chances to encounter them are higher. A general circadian regulation of ABCB1 activity has previously been shown, though the driving force behind this rhythmicity remained largely unclear (Ando et al., 2005; Kervezee et al., 2014; Zhang et al., 2009, 2018; Zhou et al., 2019). Consistently, in all these studies, the activity of ABCB1 was higher during the active phase independently of whether the active phase takes place during the dark (as for nocturnal rodents) or the light (as for diurnal species like humans) period (Zhang et al., 2009). As animals more likely encounter xenobiotics during their active period, it seems evolutionarily advantageous to pump out a foreign substance during that time of day. Similarly, we have found that the expression of *Abcb1a* and *Abcb1b* in mice was rhythmic in the LZ of the mouse placenta, peaking at the beginning of the maternal active phase.

We found that the LZ of placenta from GD15-GD15.5 fetuses expresses clock genes in a circadian manner; however, not all the considered canonical clock genes were rhythmic as they are by the end of gestation, the early neonatal life or in adult tissues. Others have shown a similar pattern of gene expression in other fetal tissues including placenta around this gestational age, indicating a not completely developed or individually variable molecular clockwork (Astiz et al., 2020; Čečmanová et al., 2019; Landgraf et al., 2015; Mészáros et al., 2014; Crew et al., 2018; Wharfe et al., 2011). However, circadian rhythmic functions could still be induced on downstream targets by early rhythmic genes (*RevErbα* and *Per2*) or by rhythmic maternal entrainment signals. In order to assess whether the local clock in the LZ is able to control the rhythmicity of ABCB1, we dissected the influence of the LZ clock from the influence of maternal GCs. When administered at high concentrations, GCs were able to induce *Abcb1a/b* expression as previously shown (Lye et al., 2018; Manceau et al., 2012). However, by using clock-deficient pregnant mice, we were able to show that constant (and physiologic) levels of maternal GC were not sufficient to drive *Abcb1a/b* rhythmic expression, which rather depended, at least partially, on the local clock in the LZ. At GD15-GD15.5 we know that circadian corticosterone levels are 10 times higher in the mother than in the fetus, showing the same circadian phase (Astiz et al., 2020). However, it has been demonstrated that, later in gestation, fetal GC production increases and that fetal and maternal GC rhythms have different phases (Torres-Farfan et al., 2011). It could therefore be possible that functions controlled by the LZ clock are dynamic during gestation and further studies might be necessary to assess the LZ clock function during other gestational windows. Maternal melatonin production also increases during late

Development (2021) 148, dev197673. doi:10.1242/dev.197673

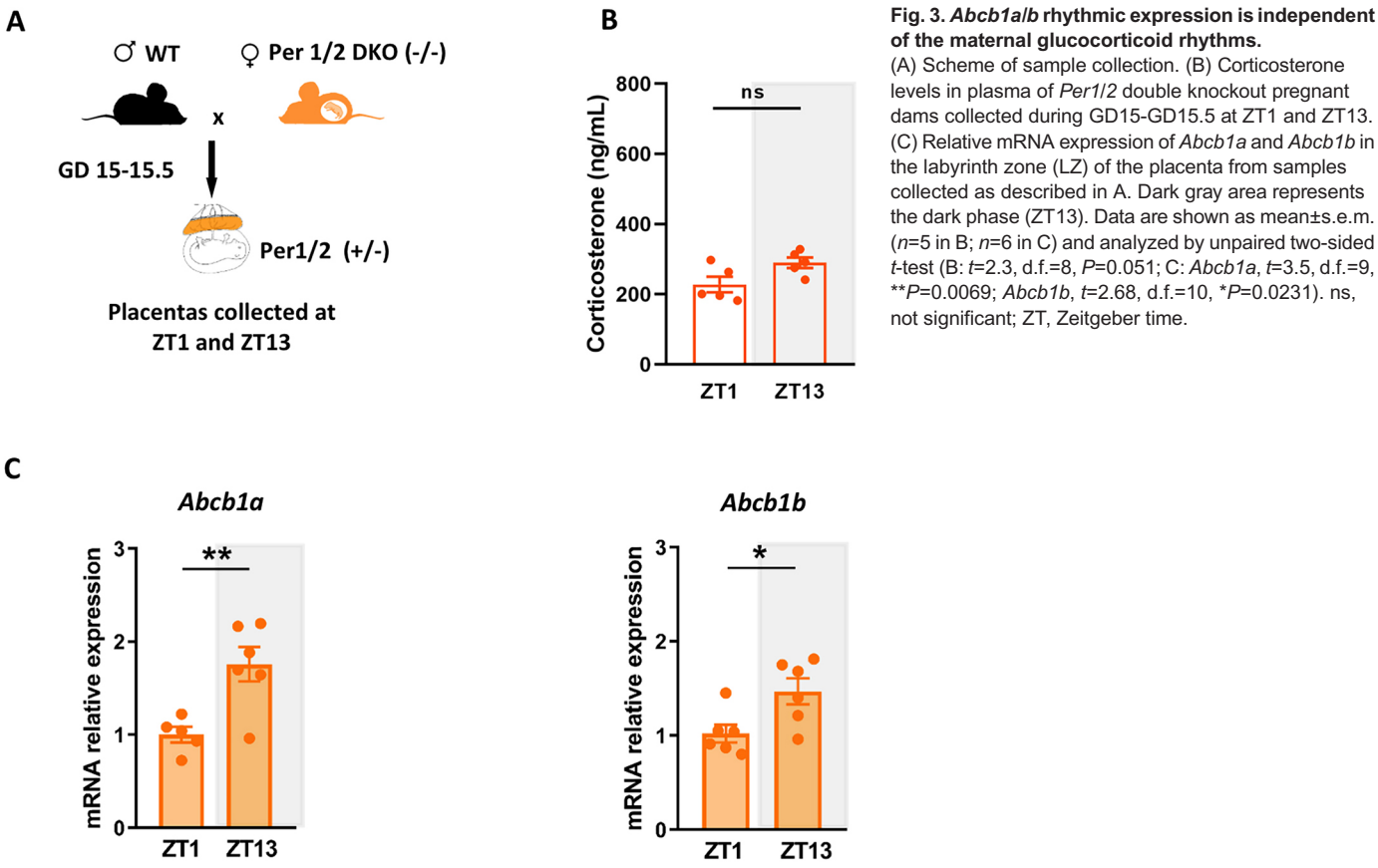

Fig. 3. *Abcb1a/b* rhythmic expression is independent of the maternal glucocorticoid rhythms. (A) Scheme of sample collection. (B) Corticosterone levels in plasma of *Per1/2* double knockout pregnant dams collected during GD15-GD15.5 at ZT1 and ZT13. (C) Relative mRNA expression of *Abcb1a* and *Abcb1b* in the labyrinth zone (LZ) of the placenta from samples collected as described in A. Dark gray area represents the dark phase (ZT13). Data are shown as mean±s.e.m. (n=5 in B; n=6 in C) and analyzed by unpaired two-sided t-test (B: t=2.3, d.f.=8, P=0.051; C: *Abcb1a*, t=3.5, d.f.=9, $^{**}P$=0.0069; *Abcb1b*, t=2.68, d.f.=10, $^{*}P$=0.0231). ns, not significant; ZT, Zeitgeber time.

gestation and, as it is robustly rhythmic and freely crosses the placenta, it has been considered as an entrainment signal for the fetal clocks (Astiz and Oster, 2021). It has been shown that the clock in the fetal SCN and the adrenal gland is responsive to maternal melatonin levels (Torres-Farfan et al., 2004, 2011; Mendez et al., 2012); however, the liver clock is not (Houdek et al., 2015). Despite

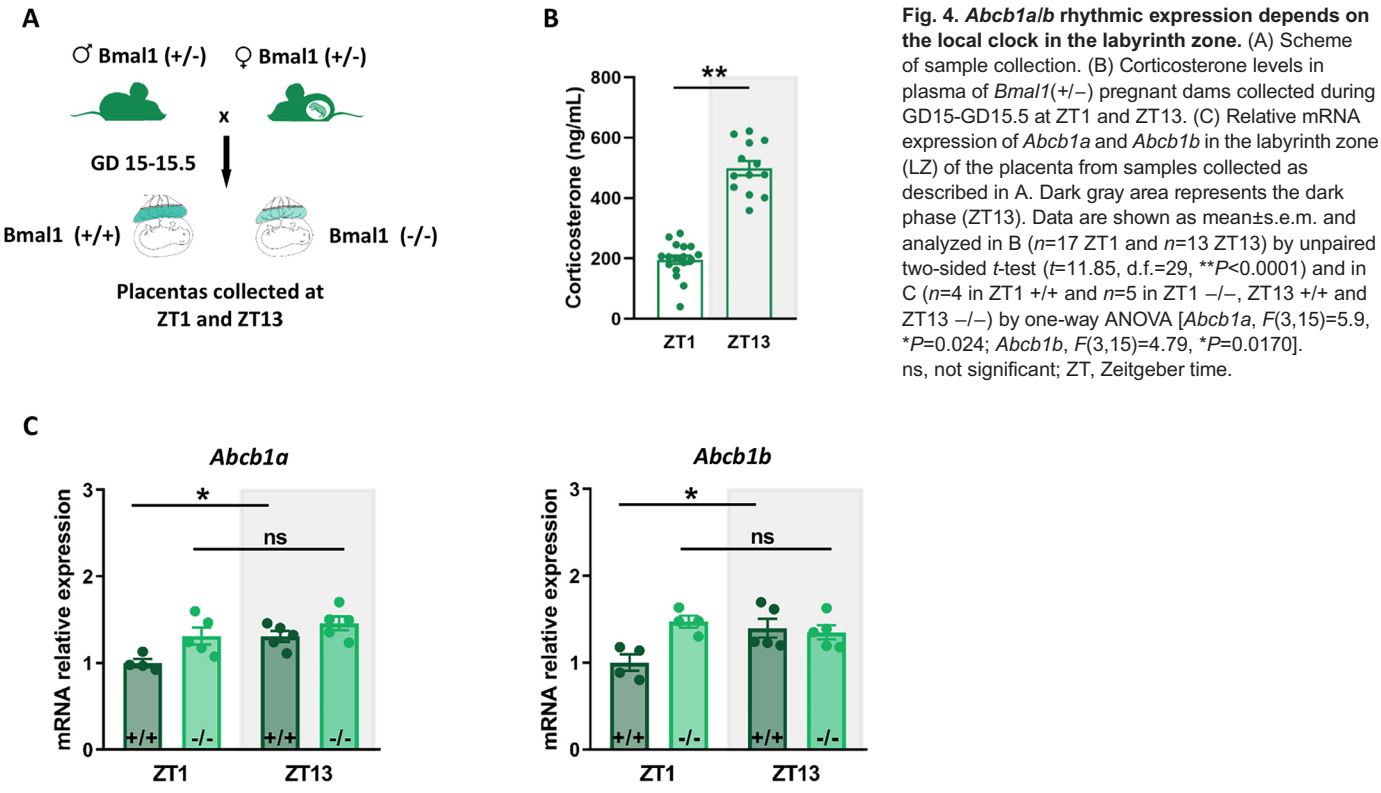

Fig. 4. *Abcb1a/b* rhythmic expression depends on the local clock in the labyrinth zone. (A) Scheme of sample collection. (B) Corticosterone levels in plasma of *Bmal1*(+/–) pregnant dams collected during GD15-GD15.5 at ZT1 and ZT13. (C) Relative mRNA expression of *Abcb1a* and *Abcb1b* in the labyrinth zone (LZ) of the placenta from samples collected as described in A. Dark gray area represents the dark phase (ZT13). Data are shown as mean±s.e.m. and analyzed in B (n=17 ZT1 and n=13 ZT13) by unpaired two-sided t-test (t=11.85, d.f.=29, $^{**}P$<0.0001) and in C (n=4 in ZT1 +/+ and n=5 in ZT1 –/–, ZT13 +/+ and ZT13 –/–) by one-way ANOVA [*Abcb1a*, F(3,15)=5.9, $^{*}P$=0.024; *Abcb1b*, F(3,15)=4.79, $^{*}P$=0.0170]. ns, not significant; ZT, Zeitgeber time.

Development (2021) 148, dev197673. doi:10.1242/dev.197673

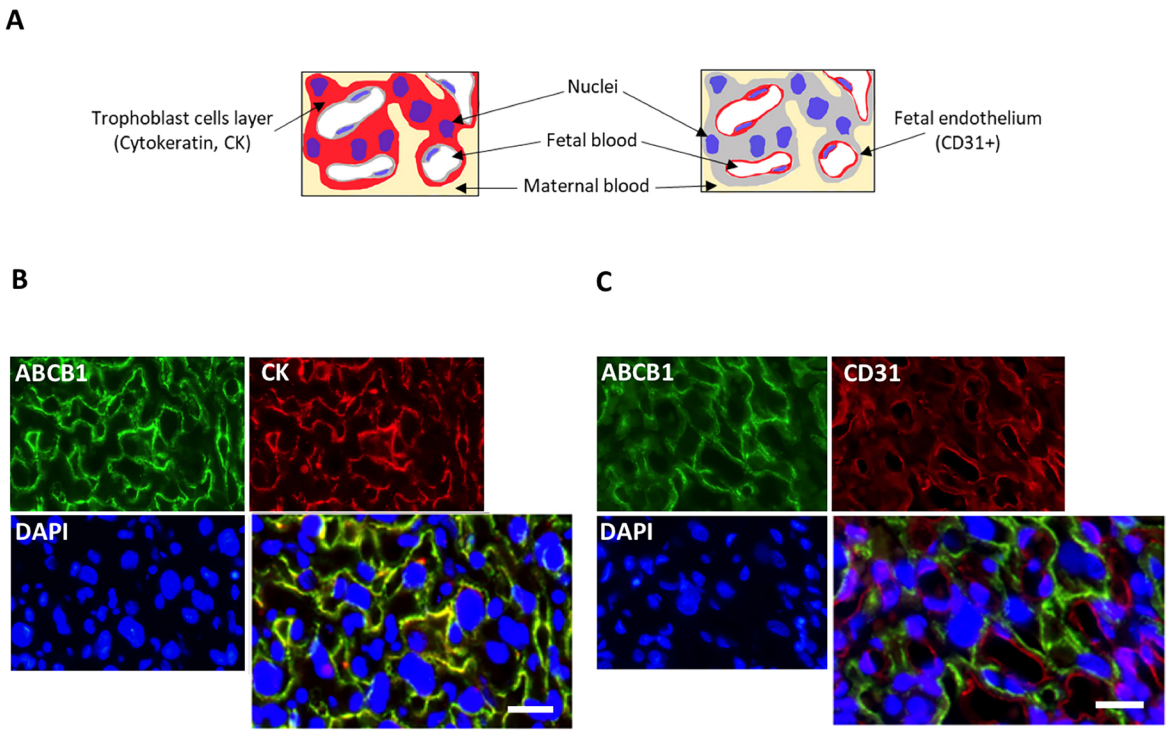

Fig. 5. ABCB1a/b is located in the trophoblasts of the labyrinth zone. (A) Scheme of the double immunofluorescence to localize ABCB1 in the labyrinth zone (LZ) of the mouse placenta, collected during GD15-GD15.5 from wild-type fetus. (B) Representative image of ABCB1 (green), cytokeratin (CK; red) used as a trophoblast marker and DAPI (blue) as a nuclear marker. (C) Representative image of ABCB1 (green), CD31 (red) used as a fetal endothelium marker and DAPI (blue) as a nuclear marker. In B and C, the bigger image on the bottom right is the merge of the three channels showing the localization of ABCB1 in the trophoblasts of the LZ. Scale bars: 10 µm.

the presence of melatonin receptors in several fetal tissues including the placenta and in different species, the sensitivity to melatonin appears to be tissue-specific (reviewed by Voiculescu et al., 2014). Unfortunately, these effects cannot be assessed in our model due to the deficient melatonin production in this mouse strain. Moreover, our study was performed in samples from male fetuses only, further studies are necessary to assess possible sex dimorphisms due to chromosomal/hormonal differences (Montano et al., 1993).

The presence of ABCB1 in the trophoblast layer allowed us to use a human cell line to further test the trophoblast clock on the rhythmic regulation of ABCB1 expression and activity. Our results showed that, although the mRNA expression and protein levels peaked 30 and 36 h after synchronization, respectively, the protein activity peaked later, possibly owing to post-translational events regulating ABCB1 traffic to the plasma membrane and/or glycosylation (Chambers et al., 1990; Conseil et al., 2001). Importantly, the activity rhythm was lost when we disrupted the clock by culturing the cells in the presence of SR8278, an antagonist of the clock protein REVERBα (Schnell et al., 2014). We and others have shown no complete correlation between Abcb1 mRNA, protein and activity levels, suggesting a likely complex interaction of regulatory mechanisms (Petropoulos et al., 2010; Zhang et al., 2018). At the transcriptional level Abcb1 expression could be modulated by the circadian activity of clock-controlled nuclear transcription factors such as HLF and E4BP4 (NFIL3) in a positive and negative manner, respectively, as previously described in the intestine (Murakami et al., 2008). A similar regulation in the LZ could explain how an immature canonical clock machinery is still able to regulate rhythmic expression of clock-controlled genes. Here, we have shown that maternal rhythms of GCs were not the main drivers of the rhythmic expression of *Abcb1* in the LZ. It could be possible that, as we have already shown in the fetal hypothalamus, the LZ clock 'gates' the amount of glucocorticoid receptor (GR) during the day through the rhythmic expression of REVERBα, which physically interacts with GR affecting its stability (Astiz et al., 2020; Okabe et al., 2016). Another possibility could be a rhythmic post-translational regulation – it is known that REVERBα is involved in the diurnal control of the glycosylation process, which is essential for the activity of ABCB1 (Wojtowicz et al., 2012). This evidence indicates that REVERBα might play an important role during the development of the fetal clocks and the maturation of circadian rhythmicity.

Drug toxicity and efficacy cannot be translated from studies performed in non-pregnant individuals as several physiological adaptations will have an impact on them, such as increased blood volume and glomerular filtration, and reduced intestinal motility (Kepley et al., 2020). Although further studies should be carried out *in vivo* as well as in other species and at other gestational periods, our results suggest that the time of day of maternal treatment with ABCB1 substrates could be an important factor to consider to avoid non-desirable effects for the fetus/mother during pregnancy.

MATERIALS AND METHODS

Mouse models and housing conditions

All mice were housed under a 12-h light, 12-h dark (LD) cycle at 22±2°C and a relative humidity of 60±5% with *ad-libitum* access to food and water (Table S1). Pregnant mice – wild-type C57BL/6J, *Per1/2* double mutant (Per1tm1BrdTyrc-Brd/J and B6.Cg-Per2tm1BrdTyrc-Brd/J) and Bmal1(+/–) [B6.129S4(Cg)-Arntltm1Weit/J on a C57BL/6J background] – were left undisturbed until maternal and fetal tissue collection on GD15-GD15.5. For mating, adult females (7-16 weeks old) from all genotypes were individually housed during only one dark phase in the presence of an experienced male. Females tend to ovulate 3-5 h after lights off, and males will copulate with

Development (2021) 148, dev197673. doi:10.1242/dev.197673

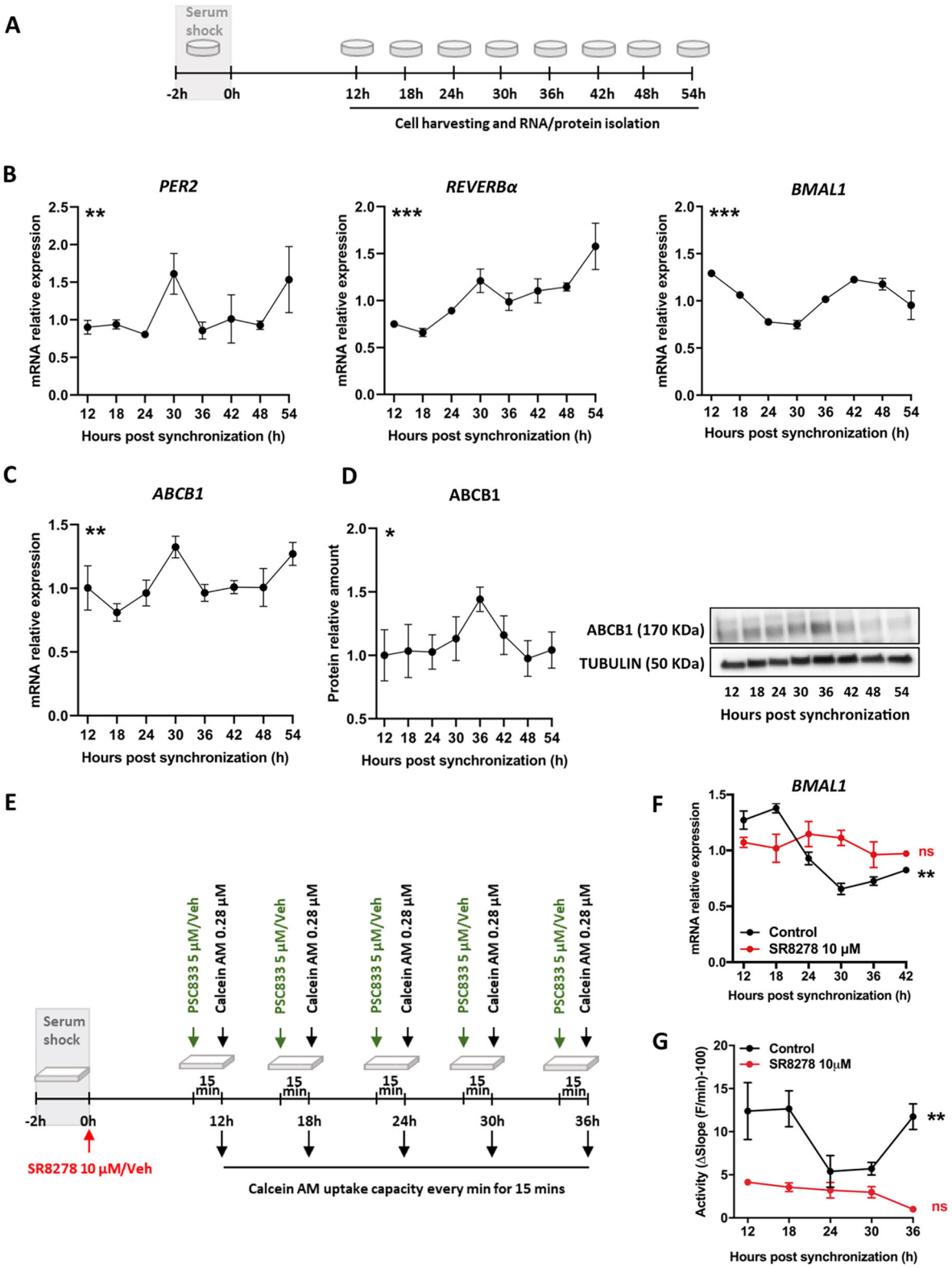

Fig. 6. The trophoblast clock controls the rhythmic expression and activity of ABCB1. (A) Scheme of the sample collection protocol. (B) mRNA relative expression of the clock genes *PER2*, *REVERBα* and *BMAL1* in samples collected as described in A. (C) mRNA relative expression of *ABCB1* in samples collected as described in A. (D) ABCB1 protein levels in BeWo cells assessed by western blot. Cells were harvested as described in A. Left: quantification of the relative amount of protein (n=6 samples/time point). Right: representative image of the PVDF membrane. Tubulin was used as a loading control. (E) Scheme of the functional assay. (F) mRNA relative expression of *BMAL1* in the presence/absence of REVERBα inhibitor SR8278 (10 µM). (G) ABCB1 activity expressed as the percentage of PSC833-sensitive transport activity at each time point. Calcein fluorescence signal was assessed in the presence/absence of REVERBα inhibitor SR8278 (10 µM). Data in B and C (n=4/time point) and D (n=6/time point) are shown as mean±s.e.m.; data in F and G are shown as mean±s.e.m. of three independent experiments performed in four (F) and five (G) technical replicates. *CircWave* software was used to assess circadian rhythmicity by fitting the data to a cosine function and *P*-values represent the statistical significance of that fit. **P*<0.05, ***P*<0.01, ****P*<0.001. ns, not significant.

Development (2021) 148, dev197673. doi:10.1242/dev.197673

them during the first half of the dark phase (Behringer et al., 2016). The next morning (GD0-GD0.5), vaginal plugs were checked and females were immediately separated and singly housed. Pregnant dams were randomly allocated to the time points of tissue collection. *Bmal1* is the only clock protein without a redundant partner, and the absence of this gene will lead to the absence of oscillations of the TTFL. However, assessing the role of the maternal clock is not possible with this mouse strain because *Bmal1* homozygous knockouts are infertile (Boden et al., 2010; Schoeller et al., 2016). *Per1* and *Per2* have complementary functions; and both genes have to be knocked out to lead to the absence of TTFL oscillations. *Per1/2* double knockout dams are fertile and allowed us to assess the function of the maternal clock when mated with wild-type males. To assess the function of the LZ clock we used *Bmal1* (+/−) heterozygous mating, resulting in 25% of the fetuses with and 25% of the fetuses without the LZ clock. *Per1/2* double heterozygous matings yielded a significantly lower percentage of fetuses of the right genotype. All experiments in mice were ethically approved by the Committee on Animal Health and Care of the Government of Schleswig-Holstein [V 242-7224.122-4(45-4/15) and V 242-7604/2017 (37-3/17] and were performed aiming to reduce the number of animals needed for the study complying with the current international guidelines on the ethical use of animals.

Tissue and plasma collection

Fifteen days after the day of the plug detection, GD15-GD15.5 females were euthanized by cervical dislocation; maternal blood and placentas were collected in 6-h intervals (ZT1, ZT7, ZT13, ZT19) or in 12-h intervals (ZT1, ZT13) according to the maternal LD cycle. We followed Zeitgeber time, ZT0 being the time when lights were switched on in the animal facility, in our case 06.00 h, and ZT12 the time when lights were switched off, in our case 18.00 h. During the times when lights were off (ZT13 and 19), mice were euthanized under red light. Corticosterone subcutaneous injections were given at a concentration of 50 mg/kg body weight. Corticosterone (Table S1) was dissolved in polyethylene glycol 400 (Table S1) at a concentration of 20 mg/mL, sonicated on ice for 2 min and sterile filtrated. Blood samples from pregnant mice were collected in EDTA-coated tubes (Table S1), plasma was obtained by centrifugation at 1500 rpm (240 ***g***) for 20 min at 4°C. Placentas only from male fetuses were kept in RNAlater (Table S1) or fixed by immersion in neutral buffered formalin [10% (v/v) formaldehyde 37% in 0.4% (w/v) NaH_2PO_4 and 0.65% (w/v) Na_2HPO_4] for 24 h (Table S1), transferred to phosphate buffer saline and embedded in paraffin blocks. For all the experiments described below, a maximum of two male fetuses per dam were included per time point and only pregnancies with at least five fetuses were included. Fetal sex and genotype were determined by PCR. Briefly, DNA from the fetal tail was isolated for 1 h at 55°C with shaking in 20 µL of 50 mM Tris (pH 8), 2 mM NaCl, 10 mM EDTA, 1% SDS containing 0.5 mg/ml of proteinase K. After 1:10 dilution with water, proteinase K was inhibited by incubation for 10 min at 95°C. Then 1 µl of DNA was used in 20 µl of PCR reaction medium containing 1× ammonium buffer, dNTPs, $MgCl_2$ and Taq polymerase (Table S1). Sex was determined by PCR (10 min at 94°C, 33 cycles of 40 s at 94°C, 60 s at 50°C, 60 s at 72°C, and finally 5 min 72°C). The presence of *IL3* indicated females (544 bp) and the presence of *IL3* (544 bp) and *SRY* (402 bp) indicated males. The following primers were used at a concentration of 20 µM: *IL-3* (5′-GGGACTCCAAGCTTCAAT-3′ and 5′-TGGAGGAGGAAGAAAAGCAA-3′) and *SRY* (5′-TGGGACTGGTG-ACAATTGTC-3′ and 5′-GAGTACAGGTGTGCAGCTCT-3′). Fetal genotype was determined by PCR for *Per1* (3 min at 94°C, 33 cycles of 30 s at 94°C, 30 s at 65°C, 1 min at 72°C and a final 10 min at 72°C), for *Per2* (15 min at 94°C, 37 cycles of 30 s at 94°C, 30 s at 55°C, 1 min at 72°C and a final 10 min at 72°C) and *Bmal1* (3 min at 94°C, 37 cycles of 30 s at 94°C, 1 min at 59°C, 1 min at 72°C and a final 5 min at 72°C). The following primers were used: *Per1* (5′-AGAACTGAGGACCCAAGCTG-3′, 5′-TT-GCCCTACAGCCTCCTGAGT-3′ and 5′-GGGGAACTTCCTGACTAG-GG-3′) giving bands of 600 bp (wild type) or 400 bp (mutant); *Per2* (5′-GAACACATCCTCATTCAAAGG-3′, 5′-CGCATGCTCCAGACTGCCT-TG-3′ and 5′-GCTGGTCCAGCTTCATCAACC-3′) giving bands of 380 bp (wild type) or 120 bp (mutant); *Bmal1* (5′-ACTGGAAGTAACTTTA-TCAAACTG-3′, 5′-CTGACCAACTTGCTAACAATTA-3′ and 5′-CTCC-TAACTTGGTTTTTGTCTGT-3′) giving bands of 330 bp (wild type) or 570 bp (mutant). A maximum of two male fetuses were used per dam.

Human trophoblast cells

Placental trophoblast (BeWo) cells of human origin were purchased from ATCC (Table S1) and cultured in Ham's F12K medium (Table S1) supplemented with 10% (v/v) FBS (Table S1) and 1% antibiotics (Table S1) and kept at 37°C and 5% CO_2. All experiments were carried out with cells in passage 9 to 20. For RNA and protein isolation, cells were plated at a density of 60,000 cells/cm^2. Then, 24 h after plating, cells were synchronized for 2 h with serum shock medium (50% F12K, 50% FBS). Twelve hours after synchronization, cells were collected every 6 h (i.e. 12, 18, 24, 30, 36, 42, 48 and 54 h post synchronization) to assess gene and protein expression during two complete cycles. The cell monolayer was washed with PBS, dried and stored at −80°C.

RNA isolation and real-time qPCR

LZ was dissected under a magnifying lens from placentas kept in RNAlater (a maximum of two per dam) until homogenization, and BeWo cells were directly homogenized with Trizol reagent and RNA isolated according to the manufacturer's instructions (Table S1). cDNA was synthesized from 1 µg RNA using a High-capacity cDNA Reverse Transcription Kit (Table S1) following the manufacturer's instructions. The cDNA was then diluted 1:10 and stored at −20°C. qPCR was performed using Go-Taq qPCR Master Mix (Table S1) with a CFX96TM thermocycler (Bio-Rad) using the following program (3 min at 95°C followed by 40 cycles of 15 s at 94°C, 15 s at 60°C and 20 s at 72°C). All samples were loaded in duplicates. Data analysis was performed using the ΔΔCT method (Livak & Schmittgen, 2001) using *B2M* (human beta-2-microglobulin) and *Eef1a1* (mouse elongation factor 1-alpha 1) as housekeeping genes after confirmation of time-independent expression and comparable amplification efficiency for every target gene. All primer sequences used are listed in Table S1.

Western blotting for Abcb1

Total protein extracts were prepared from cells homogenized with lysis buffer containing 20 mM HEPES, 100 mM NaCl, 20 mM EDTA, 5% (w/v) SDS (pH 7.4). One tablet of protease inhibitor cocktail (Table S1) was dissolved in 10 mL lysis buffer. Samples were incubated for 1 h at 50°C and centrifuged for 30 min at 13,000 rpm (18,000 ***g***) at room temperature (RT). Protein concentration was determined in the supernatant using the BCA Protein Assay Kit (Table S1). An aliquot of 50 µg of protein was incubated with loading buffer 4× containing 0.5 M Tris (pH 6.8), glycerol, 10% (w/v) SDS, β-mercaptoethanol and 0.04% (v/v) Bromophenol blue, at 42°C for 30 min. Proteins were resolved in 10% SDS polyacrylamide gels at 100 V and transferred to PVDF membranes (Table S1) at 100 V for 1.5 h. Membranes were blocked with 5% (w/v) blocker (Table S1) in 25 mM Tris (pH 7.4), 138 mM NaCl and 0.1% (v/v) Tween-20 at RT for 1 h and then incubated overnight at 4°C with monoclonal anti-Abcb1 (dilution 1:100) (Table S1). Tubulin (dilution 1:1000) was used as a loading control. Antibody reactions were visualized by enhanced chemiluminescence (ECL) (Table S1) after incubation for 1 h at RT with anti-mouse horseradish peroxidase-conjugated secondary antibody (1:3000) (Table S1). Quantification was performed using the ChemiDoc Touch Imaging System (Table S1) using the optimal auto-exposure option, to avoid undesired saturation of the signal, and quantified with Image Lab software (Table S1).

Immunohistochemistry

Paraffin-embedded placentas were sectioned using a microtome (5 µm). Central sections (determined by the presence of the umbilical cord) were used, incubated for 30 min at 60°C and re-hydrated by incubation for 10 min in Xylol, followed by 5 min in 100% ethanol, 2 min in 95%, 80%, 50% and finally washed with PBS. Endogenous peroxidase activity was inactivated by incubation with 9% (v/v) H_2O_2 in methanol (Table S1) for 20 min at RT. Sections were blocked for 20 min with 2% normal goat serum (Table S1) in PBS and incubated overnight at 4°C with rabbit anti-Bmal1 (1:250) (Table S1) in blocking solution. The day after, sections were washed three times for 10 min with PBS and incubated with a biotinylated goat anti-rabbit secondary antibody (Table S1) and amplified with ABC kit (Table S1) according to the manufacturer's instructions. The sections were developed by DAB staining (Table S1) according to the manufacturer's instructions for

Development (2021) 148, dev197673. doi:10.1242/dev.197673

2 min. Before mounting, slides were dehydrated using an ethanol series (50%, 80%, 95% and 100% ethanol solutions) for 2 min and twice for 5 min in Xylol. Slides were mounted with DPX mounting medium (Table S1). Pictures were taken at 2.5× and 10× objective using a light microscope. The number of Bmal1-positive nuclei were counted manually using a grid by an experimenter that was blinded to the time points during data collection and analysis. The total number of positive nuclei contained in 35 squares of 100 µm side were averaged for each placenta section and expressed as number of nuclei/mm^2. For each time point ZT1, ZT7, ZT13 and ZT19, placentas from six different fetuses were quantified and the results are shown as mean±s.e.m. A maximum of two male fetuses were used per dam.

Double immunofluorescence

We de-paraffinized 5 µm placenta sections and re-hydrated them as described above. An antigen retrieval step was performed by boiling the slides in sodium citrate buffer [10 mM sodium citrate (pH 6.0); Table S1] in a microwave for 3 min at 900W followed by 7 min at 270W. Sections were cooled at RT in the buffer for 30 min. A second boiling step was performed identical to the first one using new citrate buffer and cooled at RT for another 30 min. Sections were blocked for 20 min with 2% normal goat serum in PBS. Sections were incubated with primary antibodies – anti-cytokeratin (1:100) or anti-CD31 (1:50) and anti-Abcb1 (1:100) (Table S1) – overnight at 4°C. The day after, sections were washed three times for 10 min with PBS and incubated with secondary antibodies – goat anti-rabbit Alexa 594 (1:500) and goat anti-mouse Alexa 488 (1:500) (Table S1) – mixed together in a dark chamber for 1 h at RT. DAPI staining was performed to stain nuclei by incubating slides with 300 nM DAPI (Table S1) in PBS for 2 min in the dark. To minimize auto fluorescence and background, the slides were treated with True Black (Table S1) for 1.5 min before mounting with DAKO mounting medium (Table S1). Images of immunofluorescent staining were made using Nikon Ts2R-FL and identical imaging parameters for all samples.

ABCB1 activity assay

To assess ABCB1 efflux transporter activity, a calcein-AM assay previously described (Glavinas et al., 2011) was used with slight modifications. Calcein-AM is substrate of ABCB1 and ABCC1 class transporter (Olson et al., 2001), but not ABCG2 (Ivnitski-Steele et al., 2008). If no ABCB1/ABCC1 is expressed, most of the calcein-AM that passively permeates into the cells is accessible to and thus hydrolyzed by cellular esterases and becomes trapped inside the cell emitting a fluorescent signal. If ABCB1/ABCC1 is expressed, calcein-AM is exported from the plasma membrane before entering the cytosol. We have used the specific inhibitor of ABCB1 activity PCS833 (Miller et al., 2000) that leads to an increase in intracellular calcein and cellular fluorescence. The difference between the increase of fluorescence in PSC833-treated and vehicle-treated cells can be used as a measure of specific ABCB1 activity. Briefly, BeWo cells were plated at 18,500 cells/well in 96 well plates (Table S1) in Ham's F12K medium (Table S1) supplemented with 10% (v/v) FBS (Table S1) and 1% antibiotics (Table S1) and kept at 37°C and 5% CO_2. Then, 24 h after plating, cells were synchronized for 2 h with serum shock medium (50% F12K, 50% FBS). The assays were performed at 12, 18, 24, 30 and 36 h after synchronization. For each time point a separate plate was used to test the four different treatment conditions: condition 1, calcein-AM only; condition 2, calcein-AM+ABCB1 inhibitor PSC833; condition 3, calcein-AM+RevErbα inhibitor SR8278; condition 4, calcein-AM+ABCB1 inhibitor PSC833+RevErbα inhibitor SR8278. In addition, on each plate one well per group without cells was used to account for background calcein fluorescence generated by spontaneous hydrolysis. RevErbα inhibitor SR8278 (Table S1) was added at a final concentration of 10 µM at 0 h after synchronization in order to prevent circadian gene expression during the whole time frame in which ABCB1 activity was measured. SR8278 has been described previously as a specific REVERBα antagonist (Kojetin et al., 2011) and the inhibition of circadian clock gene expression has been further corroborated by several *in vivo* and *in vitro* studies (Vleira et al., 2012; Chung et al., 2014; Chatterjee et al., 2019; Lee et al., 2020; Okabe et al., 2016). The cells were quickly transferred to a plate reader (Table S1) with an atmospheric control unit (set to 37°C and 5% CO_2) 30 min before each analyzed time point. After 15 min, the ABCB1 inhibitor PSC833 (Table S1) was added at a final concentration of 5 µM using the injector function of the plate reader. After another 15 min, calcein-AM (Table S1) was added at a final concentration of 0.28 µM to all wells using the injector function of the plate reader. Directly after the last injection, calcein fluorescence reading (using the preset calcein filter settings) started. All wells were recorded in time-adjusted order after calcein-AM injection once per minute for 15 min. The focus point of reading and gain settings have been determined in pilot experiments to assure fluorescence reading of the cellular layer only. Background corrected values were used to calculate a linear positive slope of fluorescence in each well. Then, the relative fluorescence of each well from conditions 1 and 3 was calculated by using the mean value of all PSC833-treated wells from group 2 and 4, respectively. The experiment was repeated three times; each time five replicates were included per condition.

Statistical analysis

All statistical analyses were carried out using GraphPad Prism 8.0 and CircWave v1.4 and data were plotted as mean±s.e.m. Mann–Whitney (two-sided), unpaired *t*-tests (two-sided) and one-way ANOVA with Sidak's multiple-comparison test were employed as appropriate following confirmation of test assumptions. Normality was tested by Shapiro–Wilk and Kolmogorov–Smirnov tests. *P*-values below 0.05 were considered statistically significant.

Circadian rhythmicity was assessed using CircWave v1.4, which uses a Monte Carlo surrogate approach to fit a standard cosine function to an averaged de-trended data assuming a period of 24 h, a $P<0.05$ was considered a significant fit as described before (Oster et al., 2006). Sample size was determined using G-power analysis software 3.1.9.1 (University of Düsseldorf, Germany).

Acknowledgements

The authors thank Dr Sandra Blois for providing anti-cytokeratin antibody and Dr Maria Emilia Solano for providing anti-CD31 antibody and the critical reading of our paper. We thank the Institute of Neurobiology for fruitful discussions, and Nadine Oster and Ludmila Skrum for excellent technical assistance.

Competing interests

The authors declare no competing or financial interests.

Author contributions

Conceptualization: N.R., H.O., M.A.; Methodology: C.D., L.V.M.D.A., M.K., N.R., M.A.; Validation: M.A.; Formal analysis: M.K., L.V.M.D.A., M.A.; Writing - original draft: C.D., M.K., M.A.; Writing - review & editing: C.D., L.V.M.D.A., M.K., N.R., M.S., H.O., M.A.; Visualization: C.D., M.A.; Supervision: M.A.; Project administration: M.A.; Funding acquisition: H.O., M.A.

Funding

This work was supported by the Deutsche Forschungsgemeinschaft grants AS547-1/1 (to M.A.) and OS353-7/1 (to H.O.), an International Brain Research Organization-International Society for Neurochemistry research fellowship 2016 and a European Molecular Biology Organization short-term fellowship (to M.A.), and the Agencia Nacional de Promoción Científica y Tecnológica grant PICT-2016-0849 (to N.R.).

Peer review history

The peer review history is available online at https://journals.biologists.com/dev/article-lookup/DOI/10.1242/dev.197673.

References

Ando, H., Yanagihara, H., Sugimoto, K., Hayashi, Y., Tsuruoka, S., Takamura, T., Kaneko, S. and Fujimura, A. (2005). Daily rhythms of P-glycoprotein expression in mice. *Chronobiol. Int.* **22**, 655-665. doi:10.1080/07420520500180231

Astiz, M. and Oster, H. (2021). Feto-maternal crosstalk in the development of the circadian clock system. *Front. Neurosci.* **14**, 631687. doi:10.3389/fnins.2020.631687

Astiz, M., Heyde, I., Fortmann, M. I., Bossung, V., Roll, C., Stein, A., Grüttner, B., Göpel, W., Härtel, C., Obleser, J. et al. (2020). The circadian phase of antenatal glucocorticoid treatment affects the risk of behavioral disorders. *Nat. Commun.* **11**, 3593. doi:10.1038/s41467-020-17429-5

Behringer, R., Gertsenstein, M., Nagy, K. V. and Nagy, A. (2016). Selecting female mice in estrus and checking plugs. *Cold Spring Harb. Protoc.* **2016**, 729-731. doi:10.1101/pdb.prot092387

Boden, M. J., Varcoe, T. J., Voultsios, A. and Kennaway, D. J. (2010). Reproductive biology of female Bmal1 null mice. *Reproduction* **139**, 1077-1090. doi:10.1530/REP-09-0523
Borst, P. and Schinkel, A. H. (2013). P-glycoprotein ABCB1: a major player in drug handling by mammals. *J. Clin. Invest.* **123**, 4131-4133. doi:10.1172/JCI70430
Buhr, E. D. and Takahashi, J. S. (2013). Molecular components of the Mammalian circadian clock. *Handb. Exp. Pharmacol.* **217**, 3-27. doi:10.1007/978-3-642-25950-0_1
Čečmanová, V., Houdek, P., Šuchmanová, K., Sládek, M. and Sumová, A. (2019). Development and entrainment of the fetal clock in the suprachiasmatic nuclei: the role of glucocorticoids. *J. Biol. Rhythms* **34**, 307-322. doi:10.1177/0748730419835360
Chambers, T. C., Chalikonda, I. and Eilon, G. (1990). Correlation of protein kinase C translocation, P-glycoprotein phosphorylation and reduced drug accumulation in multidrug resistant human KB cells. *Biochem. Biophys. Res. Commun.* **169**, 253-259. doi:10.1016/0006-291X(90)91461-Z
Chatterjee, S., Yin, H., Li, W., Lee, J., Yechoor, V. K. and Ma, K. (2019). The nuclear receptor and clock repressor rev-erbα suppresses myogenesis. *Sci. Rep.* **9**, 4585. doi:10.1038/s41598-019-41059-7
Chourpiliadi, C. and Paparodis, R. (2020). Physiology, pituitary issues during pregnancy. In *StatPearls*. Treasure Island, FL: StatPearls Publishing.
Christ, E., Korf, H.-W. and von Gall, C. (2012). When does it start ticking? Ontogenetic development of the mammalian circadian system. *Prog. Brain Res.* **199**, 105-118. doi:10.1016/B978-0-444-59427-3.00006-X
Chung, S., Lee, E. J., Yun, S., Choe, H. K., Park, S. B., Son, H. J., Kim, K. S., Dluzen, D. E., Lee, I., Hwang, O. et al. (2014). Impact of circadian nuclear receptor REV-ERBα on midbrain dopamine production and mood regulation. *Cell* **157**, 858-868. doi:10.1016/j.cell.2014.03.039
Conseil, G., Perez-Victoria, J. M., Jault, J. M., Gamarro, F., Goffeau, A., Hofmann, J. and Di Pietro, A. (2001). Protein kinase C effectors bind to multidrug ABC transporters and inhibit their activity. *Biochemistry* **40**, 2564-2571. doi:10.1021/bi002453m
Crew, R. C., Waddell, B. J. and Mark, P. J. (2018). Obesity-induced changes in hepatic and placental clock gene networks in rat pregnancy. *Biol. Reprod.* **98**, 75-88. doi:10.1093/biolre/iox158
Dibner, C., Schibler, U. and Albrecht, U. (2010). The mammalian circadian timing system: organization and coordination of central and peripheral clocks. *Annu. Rev. Physiol.* **72**, 517-549. doi:10.1146/annurev-physiol-021909-135821
Gekakis, N., Staknis, D., Nguyen, H. B., Davis, F. C., Wilsbacher, L. D., King, D. P., Takahashi, J. S. and Weitz, C. J. (1998). Role of the CLOCK protein in the mammalian circadian mechanism. *Science* **280**, 1564-1569. doi:10.1126/science.280.5369.1564
Genovese, I., Ilari, A., Assaraf, Y. G., Fazi, F. and Colotti, G. (2017). Not only P-glycoprotein: Amplification of the ABCB1-containing chromosome region 7q21 confers multidrug resistance upon cancer cells by coordinated overexpression of an assortment of resistance-related proteins. *Drug Resist. Updat.* **32**, 23-46. doi:10.1016/j.drup.2017.10.003
Glavinas, H., von Richter, O., Vojnits, K., Mehn, D., Wilhelm, I., Nagy, T., Janossy, J., Krizbai, I., Couraud, P. and Krajcsi, P. (2011). Calcein assay: a high-throughput method to assess P-gp inhibition. *Xenobiotica* **41**, 712-719. doi:10.3109/00498254.2011.587033
Han, L. W., Gao, C. and Mao, Q. (2018). An update on expression and function of P-gp/ABCB1 and BCRP/ABCG2 in the placenta and fetus. *Expert Opin Drug Metab. Toxicol.* **14**, 817-829. doi:10.1080/17425255.2018.1499726
Honma, S. (2020). Development of the mammalian circadian clock. *Eur. J. Neurosci.* **51**, 182-193. doi:10.1111/ejn.14318
Houdek, P. and Sumová, A. (2014). In vivo initiation of clock gene expression rhythmicity in fetal rat suprachiasmatic nuclei. *PLoS ONE* **9**, e107360. doi:10.1371/journal.pone.0107360
Houdek, P., Polidarová, L., Nováková, M., Matějů, K., Kubík, Š. and Sumová, A. (2015). Melatonin administered during the fetal stage affects circadian clock in the suprachiasmatic nucleus but not in the liver. *Dev. Neurobiol.* **75**, 131-144. doi:10.1002/dneu.22213
Houdek, P., Nováková, M., Polidarová, L., Sládek, M. and Sumová, A. (2016). Melatonin is a redundant entraining signal in the rat circadian system. *Horm. Behav.* **83**, 1-5. doi:10.1016/j.yhbeh.2016.05.006
Husse, J., Eichele, G. and Oster, H. (2015). Synchronization of the mammalian circadian timing system: Light can control peripheral clocks independently of the SCN clock: alternate routes of entrainment optimize the alignment of the body's circadian clock network with external time. *BioEssays* **37**, 1119-1128. doi:10.1002/bies.201500026
Ivnitski-Steele, I., Larson, R. S., Lovato, D. M., Khawaja, H. M., Winter, S. S., Oprea, T. I., Sklar, L. A. and Edwards, B. S. (2008). High-throughput flow cytometry to detect selective inhibitors of ABCB1, ABCC1, and ABCG2 transporters. *Assay Drug Dev. Technol.* **6**, 263-276. doi:10.1089/adt.2007.107
Kepley, J. M., Bates, K. and Mohiuddin, S. S. (2020). Physiology, maternal changes. In *StatPearls*, Treasure Island, FL: StatPearls Publishing.
Kervezee, L., Hartman, R., van den Berg, D.-J., Shimizu, S., Emoto-Yamamoto, Y., Meijer, J. H. and de Lange, E. C. M. (2014). Diurnal variation in P-glycoprotein-mediated transport and cerebrospinal fluid turnover in the brain. *AAPS J.* **16**, 1029-1037. doi:10.1208/s12248-014-9625-4
Kojetin, D., Wang, Y., Kamenecka, T. M. and Burris, T. P. (2011). Identification of SR8278, a synthetic antagonist of the nuclear heme receptor REV-ERB. *ACS Chem. Biol.* **6**, 131-134. doi:10.1021/cb1002575
Krozowski, Z., Li, K. X., Koyama, K., Smith, R. E., Obeyesekere, V. R., Stein-Oakley, A., Sasano, H., Coulter, C., Cole, T. and Sheppard, K. E. (1999). The type I and type II 11beta-hydroxysteroid dehydrogenase enzymes. *J. Steroid Biochem. Mol. Biol.* **69**, 391-401. doi:10.1016/S0960-0760(99)00074-6
Landgraf, D., Achten, C., Dallmann, F. and Oster, H. (2015). Embryonic development and maternal regulation of murine circadian clock function. *Chronobiol. Int.* **32**, 416-427. doi:10.3109/07420528.2014.986576
Lee, J., Kim, D. E., Griffin, P., Sheehan, P. W., Kim, D. H., Musiek, E. S. and Yoon, S. Y. (2020). Inhibition of REV-ERBs stimulates microglial amyloid-beta clearance and reduces amyloid plaque deposition in the 5XFAD mouse model of Alzheimer's disease. *Aging Cell* **19**, e13078. doi:10.1111/acel.13078
Li, Y., Gonzalez, P. and Zhang, L. (2012). Fetal stress and programming of hypoxic/ischemic-sensitive phenotype in the neonatal brain: mechanisms and possible interventions. *Prog. Neurobiol.* **98**, 145-165. doi:10.1016/j.pneurobio.2012.05.010
Livak, K. and Schmittgen, T. (2001). Analysis of relative gene expression data using real-time quantitative PCR and the 2(-Delta Delta C(T)) Method. *Methods* **25**, 402-408. doi:10.1006/meth.2001.1262
Lye, P., Bloise, E., Nadeem, L., Gibb, W., Lye, S. J. and Matthews, S. G. (2018). Glucocorticoids modulate multidrug resistance transporters in the first trimester human placenta. *J. Cell. Mol. Med.* **22**, 3652-3660. doi:10.1111/jcmm.13646
Manceau, S., Giraud, C., Declèves, X., Scherrmann, J. M., Artiguebieille, F., Goffinet, F., Chappuy, H., Vinot, C. and Tréluyer, J. M. (2012). ABC drug transporter and nuclear receptor expression in human cytotrophoblasts: influence of spontaneous syncytialization and induction by glucocorticoids. *Placenta* **33**, 927-932. doi:10.1016/j.placenta.2012.07.016
Mark, P. J., Crew, R. C., Wharfe, M. D. and Waddell, B. J. (2017). Rhythmic Three-part harmony: the complex interaction of maternal, placental and fetal circadian Systems. *J. Biol. Rhythms* **32**, 534-549. doi:10.1177/0748730417728671
Mendez, N., Abarzua-Catalan, L., Vilches, N., Galdames, H. A., Spichiger, C., Richter, H. G., Valenzuela, G. J., Seron-Ferre, M. and Torres-Farfan, C. (2012). Timed maternal melatonin treatment reverses circadian disruption of the fetal adrenal clock imposed by exposure to constant light. *PLoS ONE* **7**, e42713. doi:10.1371/journal.pone.0042713
Mendez, N., Halabi, D., Spichiger, C., Salazar, E. R., Vergara, K., Alonso-Vasquez, P., Carmona, P., Sarmiento, J. M., Richter, H. G., Seron-Ferre, M. et al. (2016). Gestational chronodisruption impairs circadian physiology in rat male offspring, increasing the risk of chronic disease. *Endocrinology* **157**, 4654-4668. doi:10.1210/en.2016-1282
Mészáros, K., Pruess, L., Szabó, A. J., Gondan, M., Ritz, E. and Schaefer, F. (2014). Development of the circadian clockwork in the kidney. *Kidney Int.* **86**, 915-922. doi:10.1038/ki.2014.199
Miller, D. S., Nobmann, S. N., Gutmann, H., Toeroek, M., Drewe, J. and Fricker, G. (2000). Xenobiotic transport across isolated brain microvessels studied by confocal microscopy. *Mol. Pharmacol.* **58**, 1357-1367. doi:10.1124/mol.58.6.1357
Montano, M. M., Wang, M.-H. and vom Saal, F. S. (1993). Sex differences in plasma corticosterone in mouse fetuses are mediated by differential placental transport from the mother and eliminated by maternal adrenalectomy or stress. *Reprod Fertil* **99**, 283-290. doi:10.1530/jrf.0.0990283
Murakami, Y., Higashi, Y., Matsunaga, N., Koyanagi, S. and Ohdo, S. (2008). Circadian clock-controlled intestinal expression of the multidrug-resistance gene mdr1a in mice. *Gastroenterology* **135**, 1636-1644.e3. doi:10.1053/j.gastro.2008.07.073
Novotna, M., Libra, A., Kopecky, M., Pavek, P., Fendrich, Z., Semecky, V. and Staud, F. (2004). P-glycoprotein expression and distribution in the rat placenta during pregnancy. *Reprod. Toxicol.* **18**, 785-792. doi:10.1016/j.reprotox.2004.04.014
Okabe, T., Chavan, R., Fonseca Costa, S. S., Brenna, A., Ripperger, J. A. and Albrecht, U. (2016). REV-ERBα influences the stability and nuclear localization of the glucocorticoid receptor. *J. Cell Sci.* **129**, 4143-4154. doi:10.1242/jcs.190959
Okatani, Y., Okamoto, K., Hayashi, K., Wakatsuki, A., Tamura, S. and Sagara, Y. (1998). Maternal-fetal transfer of melatonin in pregnant women near term. *J. Pineal Res.* **25**, 129-134. doi:10.1111/j.1600-079X.1998.tb00550.x
Olson, D. P., Taylor, B. J. and Ivy, S. P. (2001). Detection of MRP functional activity: calcein AM but not BCECF AM as a Multidrug Resistance-related Protein (MRP1) substrate. *Cytometry* **46**:105-113. doi:10.1002/cyto.1072
Oster, H., Damerow, S., Hut, R. A. and Eichele, G. (2006). Transcriptional profiling in the adrenal gland reveals circadian regulation of hormone biosynthesis genes and nucleosome assembly genes. *J. Biol. Rhythms* **21**, 350-361. doi:10.1177/0748730406293053
Papacleovoulou, G., Nikolova, V., Oduwole, O., Chambers, J., Vazquez-Lopez, M., Jansen, E., Nicolaides, K., Parker, M. and Williamson, C. (2017). Gestational disruptions in metabolic rhythmicity of the liver, muscle, and placenta affect fetal size. *FASEB J.* **31**, 1698-1708. doi:10.1096/fj.201601032R

Petropoulos, S., Gibb, W. and Matthews, S. G. (2010). Effect of glucocorticoids on regulation of placental multidrug resistance phosphoglycoprotein (P-gp) in the mouse. *Placenta* **31**, 803-810. doi:10.1016/j.placenta.2010.06.014

Ralph, M. R., Foster, R. G., Davis, F. C. and Menaker, M. (1990). Transplanted suprachiasmatic nucleus determines circadian period. *Science* **247**, 975-978. doi:10.1126/science.2305266

Reppert, S. M. and Schwartz, W. J. (1984). The suprachiasmatic nuclei of the fetal rat: characterization of a functional circadian clock using 14C-labeled deoxyglucose. *J. Neurosci.* **4**, 1677-1682. doi:10.1523/JNEUROSCI.04-07-01677.1984

Russell, J. A. and Brunton, P. J. (2019). Giving a good start to a new life via maternal brain allostatic adaptations in pregnancy. *Front. Neuroendocrinol.* **53**, 100739. doi:10.1016/j.yfrne.2019.02.003

Schibler, U., Ripperger, J. and Brown, S. A. (2003). Peripheral circadian oscillators in mammals: time and food. *J. Biol. Rhythms* **18**, 250-260. doi:10.1177/0748730403018003007

Schnell, A., Chappuis, S., Schmutz, I., Brai, E., Ripperger, J. A., Schaad, O., Welzl, H., Descombes, P., Alberi, L. and Albrecht, U. (2014). The nuclear receptor REV-ERBα regulates Fabp7 and modulates adult hippocampal neurogenesis. *PLoS ONE* **9**, e99883. doi:10.1371/journal.pone.0099883

Schoeller, E. L., Clark, D. D., Dey, S., Cao, N. V., Semaan, S. J., Chao, L. W., Kauffman, A. S., Stowers, L. and Mellon, P. L. (2016). Bmal1 is required for normal reproductive behaviors in male mice. *Endocrinology* **157**, 4914-4929. doi:10.1210/en.2016-1620

Serón-Ferré, M., Mendez, N., Abarzua-Catalan, L., Vilches, N., Valenzuela, F. J., Reynolds, H. E., Llanos, A. J., Rojas, A., Valenzuela, G. J. and Torres-Farfan, C. (2012). Circadian rhythms in the fetus. *Mol. Cell. Endocrinol.* **349**, 68-75. doi:10.1016/j.mce.2011.07.039

Shearman, L. P., Sriram, S., Weaver, D. R., Maywood, E. S., Chaves, I., Zheng, B., Kume, K., Lee, C. C., van der Horst, G. T., Hastings, M. H. et al. (2000). Interacting molecular loops in the mammalian circadian clock. *Science* **288**, 1013-1019. doi:10.1126/science.288.5468.1013

Sibley, C. and Dilworth, M. (2020). 8 - Placental Function in Maternofetal Exchange. In *Fetal Medicine*, 3rd edn (ed. P. P. Pandya, D. Oepkes, N. J. Sebire and R. J. Wapner), pp. 69-77.e2. London: Content Repository Only!.

Smarr, B. L., Grant, A. D., Perez, L., Zucker, I. and Kriegsfeld, L. J. (2017). Maternal and early-life circadian disruption have long-lasting negative consequences on offspring development and adult behavior in mice. *Sci. Rep.* **7**, 3326. doi:10.1038/s41598-017-03406-4

So, A. Y.-L., Bernal, T. U., Pillsbury, M. L., Yamamoto, K. R. and Feldman, B. J. (2009). Glucocorticoid regulation of the circadian clock modulates glucose homeostasis. *Proc. Natl. Acad. Sci. USA* **106**, 17582-17587. doi:10.1073/pnas.0909733106

Staud, F. and Karahoda, R. (2018). Trophoblast: The central unit of fetal growth, protection and programming. *Int. J. Biochem. Cell Biol.* **105**, 35-40. doi:10.1016/j.biocel.2018.09.016

Sun, M., Kingdom, J., Baczyk, D., Lye, S. J., Matthews, S. G. and Gibb, W. (2006). Expression of the multidrug resistance P-glycoprotein, (ABCB1 glycoprotein) in the human placenta decreases with advancing gestation. *Placenta* **27**, 602-609. doi:10.1016/j.placenta.2005.05.007

Takahashi, J. S. (2017). Transcriptional architecture of the mammalian circadian clock. *Nat. Rev. Genet.* **18**, 164-179. doi:10.1038/nrg.2016.150

Torres-Farfan, C., Richter, H. G., Germain, A. M., Valenzuela, G. J., Campino, C., Rojas-García, P., Forcelledo, M. L., Torrealba, F. and Serón-Ferré, M. (2004). Maternal melatonin selectively inhibits cortisol production in the primate fetal adrenal gland. *J. Physiol* **554**, 841-856. doi:10.1113/jphysiol.2003.056465

Torres-Farfan, C., Mendez, N., Abarzua-Catalan, L., Vilches, N., Valenzuela, G. J. and Seron-Ferre, M. (2011). A circadian clock entrained by melatonin is ticking in the rat fetal adrenal. *Endocrinology* **152**:1891-1900. doi:10.1210/en.2010-1260

Varcoe, T. J., Wight, N., Voultsios, A., Salkeld, M. D. and Kennaway, D. J. (2011). Chronic phase shifts of the photoperiod throughout pregnancy programs glucose intolerance and insulin resistance in the rat. *PLoS ONE* **6**, e18504. doi:10.1371/journal.pone.0018504

Varcoe, T. J., Boden, M. J., Voultsios, A., Salkeld, M. D., Rattanatray, L. and Kennaway, D. J. (2013). Characterisation of the maternal response to chronic phase shifts during gestation in the rat: implications for fetal metabolic programming. *PLoS ONE* **8**, e53800. doi:10.1371/journal.pone.0053800

Varcoe, T. J., Gatford, K. L. and Kennaway, D. J. (2018). Maternal circadian rhythms and the programming of adult health and disease. *Am. J. Physiol. Regul. Integr. Comp. Physiol.* **314**, R231-R241. doi:10.1152/ajpregu.00248.2017

Vieira, E., Marroquí, L., Batista, T. M., Caballero-Garrido, E., Carneiro, E. M., Boschero, A. C., Nadal, A. and Quesada, I. (2012). The clock gene Rev-erbα regulates pancreatic β-cell function: modulation by leptin and high-fat diet. *Endocrinology* **153**, 592-601. doi:10.1210/en.2011-1595

Vilches, N., Spichiger, C., Mendez, N., Abarzua-Catalan, L., Galdames, H. A., Hazlerigg, D. G., Richter, H. G. and Torres-Farfan, C. (2014). Gestational chronodisruption impairs hippocampal expression of NMDA receptor subunits Grin1b/Grin3a and spatial memory in the adult offspring. *PLoS ONE* **9**, e91313. doi:10.1371/journal.pone.0091313

Voiculescu, S. E., Zygouropoulos, N., Zahiu, C. D. and Zagrean, A. M. (2014). Role of melatonin in embryo fetal development. *J. Med. Life* **7**, 488-492.

Waddell, B. J., Wharfe, M. D., Crew, R. C. and Mark, P. J. (2012). A rhythmic placenta? Circadian variation, clock genes and placental function. *Placenta* **33**, 533-539. doi:10.1016/j.placenta.2012.03.008

Wharfe, M. D., Mark, P. J. and Waddell, B. J. (2011). Circadian variation in placental and hepatic clock genes in rat pregnancy. *Endocrinology* **152**, 3552-3560. doi:10.1210/en.2011-0081

Wharfe, M. D., Mark, P. J., Wyrwoll, C. S., Smith, J. T., Yap, C., Clarke, M. W. and Waddell, B. J. (2016). Pregnancy-induced adaptations of the central circadian clock and maternal glucocorticoids. *J. Endocrinol.* **228**, 135-147. doi:10.1530/JOE-15-0405

Wojtowicz, K., Szaflarski, W., Januchowski, R., Zawierucha, P., Nowicki, M. and Zabel, M. (2012). Inhibitors of N-glycosylation as a potential tool for analysis of the mechanism of action and cellular localisation of glycoprotein P. *Acta Biochim. Pol.* **59**, 445-450. doi:10.18388/abp.2012_2076

Zhang, Y.-K. J., Yeager, R. L. and Klaassen, C. D. (2009). Circadian expression profiles of drug-processing genes and transcription factors in mouse liver. *Drug Metab. Dispos.* **37**, 106-115. doi:10.1124/dmd.108.024174

Zhang, S. L., Yue, Z., Arnold, D. M., Artiushin, G. and Sehgal, A. (2018). A circadian clock in the blood-brain barrier regulates xenobiotic efflux. *Cell* **173**, 130-139.e10. doi:10.1016/j.cell.2018.02.017

Zhou, C., Yu, F., Zeng, P., Zhang, T., Huang, H., Chen, W. and Wu, B. (2019). Circadian sensitivity to the cardiac glycoside oleandrin is associated with diurnal intestinal P-glycoprotein expression. *Biochem. Pharmacol.* **169**, 113622. doi:10.1016/j.bcp.2019.08.024